AD-A037 672 SOUTHWEST RESEARCH INST SAN ANTONIO TEX F/G 11/6
NONDESTRUCTIVE EVALUATION OF METAL FATIGUE.(U)
FEB 77 F N KUSENBERGER, G A MATZKANIN F44620-75-C-0042
UNCLASSIFIED SWRI-15-4163 AFOSR-TR-77-0191 NL

| OF |
AD
A037672

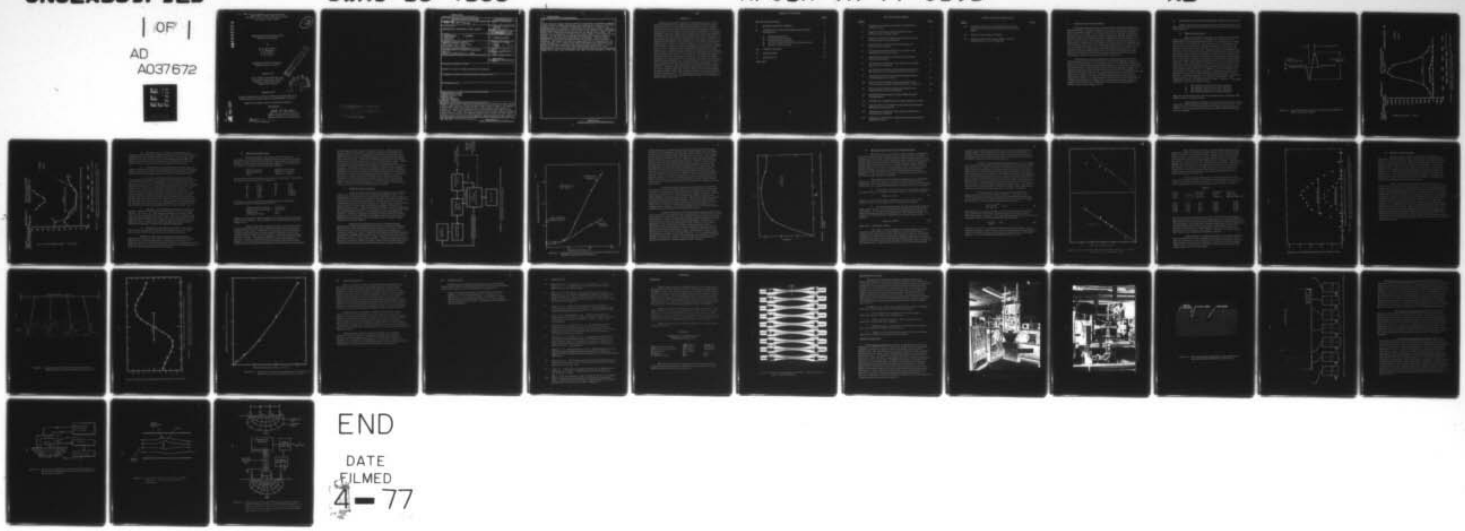

END

DATE
FILMED
4-77

SOUTHWEST RESEARCH INSTITUTE
Post Office Drawer 28510, 8500 Culebra Road
San Antonio, Texas 78284

12

NONDESTRUCTIVE EVALUATION OF METAL FATIGUE

by

F. N. Kusenberger
G. A. Matzkanin
J. R. Barton
P. H. Francis

INTERIM SCIENTIFIC REPORT
SwRI Project No. 15-4163

Prepared for

A. F. Office of Scientific Research
Directorate of Aerospace Sciences
Contract F44620-75-C-0042
Project No. 9782-05

February 1977

Research Sponsored by Air Force Office of Scientific Research
Directorate of Aerospace Sciences, United States Air Force

APPROVED:

John R. Barton

John R. Barton, Vice President
Instrumentation Research Division

AIR FORCE OFFICE OF SCIENTIFIC RESEARCH (AFSC)
NOTICE OF TRANSMITTAL TO DDC
This technical report has been reviewed and is approved for public release IAW AFR 190-12 (7b).
Distribution is unlimited.
A. D. BLOSE
Technical Information Officer

UNCLASSIFIED

SECURITY CLASSIFICATION OF THIS PAGE (When Data Entered)

REPORT DOCUMENTATION PAGE	READ INSTRUCTIONS BEFORE COMPLETING FORM
1. REPORT NUMBER: AFOSR - TR - 77 - 0191	2. GOVT ACCESSION NO.
3. RECIPIENT'S CATALOG NUMBER	
4. TITLE (and Subtitle): NONDESTRUCTIVE EVALUATION OF METAL FATIGUE	5. TYPE OF REPORT & PERIOD COVERED: INTERIM rept. Jan 76 - Dec 76
6. PERFORMING ORG. REPORT NUMBER: SwRI Project No. 15-4163	
7. AUTHOR(s): F. N. KUSENBERGER, J. R. BARTON, G. A. MATZKANIN, P. H. FRANCIS	8. CONTRACT OR GRANT NUMBER(s): F44620-75-C-0042
9. PERFORMING ORGANIZATION NAME AND ADDRESS: SOUTHWEST RESEARCH INSTITUTE, 8500 Culebra Rd, PO Drawer 28510, SAN ANTONIO, TEXAS 78284	10. PROGRAM ELEMENT, PROJECT, TASK AREA & WORK UNIT NUMBERS: 9782, 2307B2, 61102F
11. CONTROLLING OFFICE NAME AND ADDRESS: AIR FORCE OFFICE OF SCIENTIFIC RESEARCH/NA, BLDG 410, BOLLING AIR FORCE BASE, D C 20332	12. REPORT DATE: Feb 77
	13. NUMBER OF PAGES: 40
14. MONITORING AGENCY NAME & ADDRESS (if different from Controlling Office)	15. SECURITY CLASS. (of this report): UNCLASSIFIED
	15a. DECLASSIFICATION/ DOWNGRADING SCHEDULE

16. DISTRIBUTION STATEMENT (of this Report)

Approved for public release; distribution unlimited.

17. DISTRIBUTION STATEMENT (of the abstract entered in Block 20, if different from Report)

18. SUPPLEMENTARY NOTES

19. KEY WORDS (Continue on reverse side if necessary and identify by block number)

NONDESTRUCTIVE TESTING
MAGNETIC LEAKAGE FIELD
FATIGUE TESTS
FRACTURE MECHANICS
MAGNETIC INSPECTION

20. ABSTRACT (Continue on reverse side if necessary and identify by block number)

Magnetic perturbation signatures and Barkhausen noise results have been obtained from an AISI 4340 steel fatigue specimen stress-cycled at 180ksi. The magnetic perturbation signals were obtained over a large number an scan tracks for a variety of applied load conditions and for crack lengths from 0.010 inch to 0.050 inch. The signal amplitude varies with load and crack length in agreement with analytical results for magnetic leakage fields, whereas the signal shape appears to be related to the crack depth and localized plastic zones. Analysis of the magnetic perturbation data suggests a crack opening model for small

DD FORM 1 JAN 73 1473 EDITION OF 1 NOV 65 IS OBSOLETE

UNCLASSIFIED 328 200

SECURITY CLASSIFICATION OF THIS PAGE (When Data Ent.

surface entering fatigue cracks in which the crack opens in response to applied external forces as though the adjacent crack surfaces are hinged at the bottom. Analytical work is in progress to interpret these results in terms of the magneto-mechanical properties in the vicinity of the fatigue crack. Barkhausen noise signals were obtained on a grid pattern in the vicinity of several fatigue cracks with a Barkhausen detection probe 1/5 the length of the cracks. The results can be interpreted in terms of the stress fields in the vicinity of the cracks. AF 1410 steel fatigue specimens are being fabricated for magnetic perturbation and Barkhausen noise analysis measurements. Fatigue cracks in Ti-6Al-4V specimens were investigated with the electric current injection technique. The results show that the singal amplitude is correlated with the crack interface area. Fatigue crack depth measurements were also made on the Ti-6Al-4V specimen using the AC four-contact electric probe method. A micro-miniature probe with 0.010 inch contact spacing was developed for these measurements. The results agree well with the predictions of electric potential theory and indicate that the fatigue crack depth can be determined to within 10%.

ABSTRACT

Magnetic perturbation signatures and Barkhausen noise results have been obtained from an AISI 4340 steel fatigue specimen stress-cycled at 180 ksi. The magnetic perturbation signals were obtained over a large number of scan tracks for a variety of applied load conditions and for crack lengths from 0.010 inch to 0.050 inch. The signal amplitude varies with load and crack length in agreement with analytical results for magnetic leakage fields, whereas the signal shape appears to be related to the crack depth and localized plastic zones. Analysis of the magnetic perturbation data suggests a crack opening model for small surface entering fatigue cracks in which the crack opens in response to applied external forces as though the adjacent crack surfaces are hinged at the bottom. Analytical work is in progress to interpret these results in terms of the magneto-mechanical properties in the vicinity of the fatigue crack. Barkhausen noise signals were obtained on a grid pattern in the vicinity of several fatigue cracks with a Barkhausen detection probe 1/5 the length of the cracks. The results can be interpreted in terms of the stress fields in the vicinity of the cracks. AF 1410 steel fatigue specimens are being fabricated for magnetic perturbation and Barkhausen noise analysis measurements. Fatigue cracks in Ti-6Al-4V specimens were investigated with the electric current injection technique. The results show that the signal amplitude is correlated with the crack interface area. Fatigue crack depth measurements were also made on the Ti-6Al-4V specimen using the AC four-contact electric probe method. A micro-miniature probe with 0.010 inch contact spacing was developed for these measurements. The results agree well with the predictions of electric potential theory and indicate that the fatigue crack depth can be determined to within 10%.

TABLE OF CONTENTS

LIST OF ILLUSTRATIONS

LIST OF ILLUSTRATIONS (Contd.)

I. INTRODUCTION AND SUMMARY

Investigation has continued of the quantitative functional relationships between magnetic perturbation signatures and crack parameters of interest for fracture mechanics analysis, such as, crack length, crack opening displacement (COD), crack depth, crack interface area, crack opening configuration, and void volume. Efforts have continued to determine possible relationships between signal features and plastic zone configuration around a fatigue crack. Work this past year has also emphasized residual stress measurements as determined by Barkhausen noise analysis, AC four-contact probe measurements of crack depth, and electric current injection measurements of crack interface size in titanium alloy specimens. Work has proceeded on an automatic monitoring and data processing capability for the stress-cycling machine. The automatic feature will eliminate the need for continuous manual monitoring during the extended stress-cycling necessary for generating fatigue cracks in specimens of electro-vacuum processed AF 1410 steel.

The following sections in this Report briefly summarize the results obtained during the past year utilizing the various NDE methods mentioned above (a brief description of the methods is given in the Appendix). Significant progress has been made in applying the Barkhausen noise analysis method and the AC four-contact electric probe method to the investigation of fatigue cracks. Results obtained with these methods are being used to aid in the analysis of magnetic perturbation and electric current injection data. In addition, analytical work is proceeding in efforts to interpret characteristics of the magnetic perturbation signature in terms of the magneto-mechanical features of the fatigue crack region. As explained later, analyses of our recent data suggests a significant development, namely that a crack opening model in which the adjacent crack surfaces are "hinged" at the bottom may be appropriate for small surface entering fatigue cracks.

II. EXPERIMENTAL INVESTIGATIONS AND SUMMARY OF RESULTS

Details regarding the specimen geometry and characteristics, the NDE methods employed, and the general experimental procedure are given in the Appendix.

A. Magnetic Perturbation

Magnetic Perturbation signals were obtained on rod-shaped fatigue specimens by utilizing a small Hall probe to detect the field perturbations associated with fatigue cracks. The Hall probe was made to traverse a precise path along the specimen axis (perpendicular to the crack interface) by means of a scanning mechanism. The width of the scan track interrogated by the Hall probe is not precisely known but is probably no more than 0.002 inch. Extensive magnetic perturbation data were taken on a specimen of AISI 4340 steel which had been stress-cycled in tension using a zero to peak stress of 180 ksi with a stress ratio R = 0. The stress-cycling machine was stopped at various crack lengths ranging from 0.010 inch to 0.050 inch, and magnetic perturbation measurements were made at five values of applied static stress up to a maximum stress of 180 ksi. Data were obtained with the specimen magnetized nearly to saturation using a magnetizing current of 6.0 ampere (referred to as the "high field", or HF, condition) and also at a lower magnetizing current of 0.8 ampere ("low field", or LF, condition). For each condition of crack length and applied stress, magnetic perturbation signatures were obtained from a number of adjacent traske perpendicular to the crack interface. Typical signatures from various locations along a crack interface are shown in the Appendix. As previously reported[1], a two-component signature was observed such as shown in Figure 1. The signal parameters extracted for analysis were:

1. The principal signal peak-to-peak amplitude.
2. The satellite signal peak-to-peak amplitude.
3. The principal signal peak-to-peak separation.
4. The satellite signal peak-to-peak separation.

All of the recorded data were reduced and plotted using a Tektronix 4051 BASIC Graphic Computing System.

Representative results for the variation along the crack interface of the signal amplitude and width are shown in Figures 2 and 3. These results are for a 0.052 inch long fatigue crack with an applied stress of 180 ksi. An overall appraisal of the magnetic data leads to the following summary results:

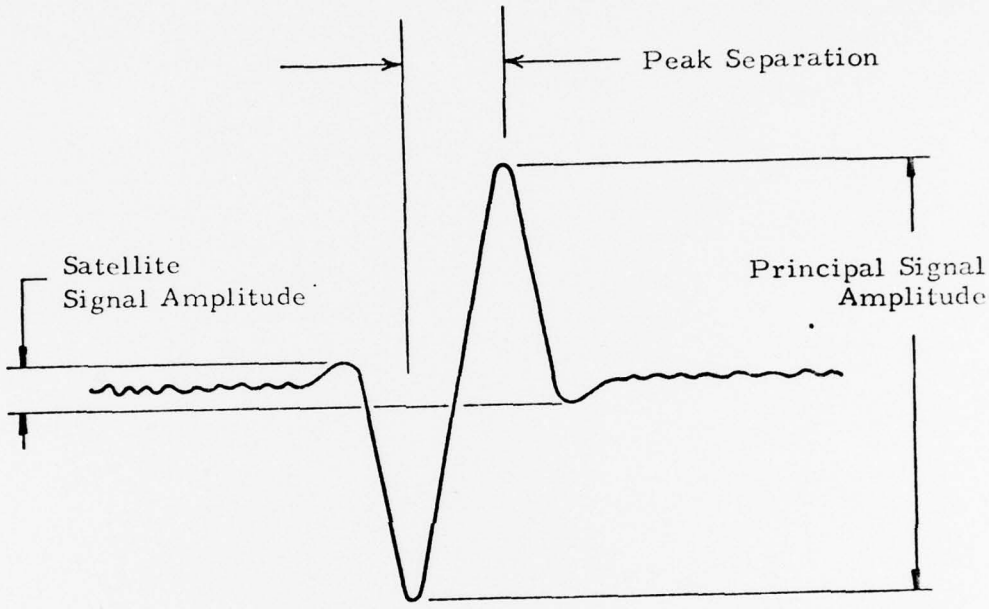

3059

FIGURE 1. CHARACTERISTIC MAGNETIC SIGNATURE ASSOCIATED WITH A SURFACE CRACK

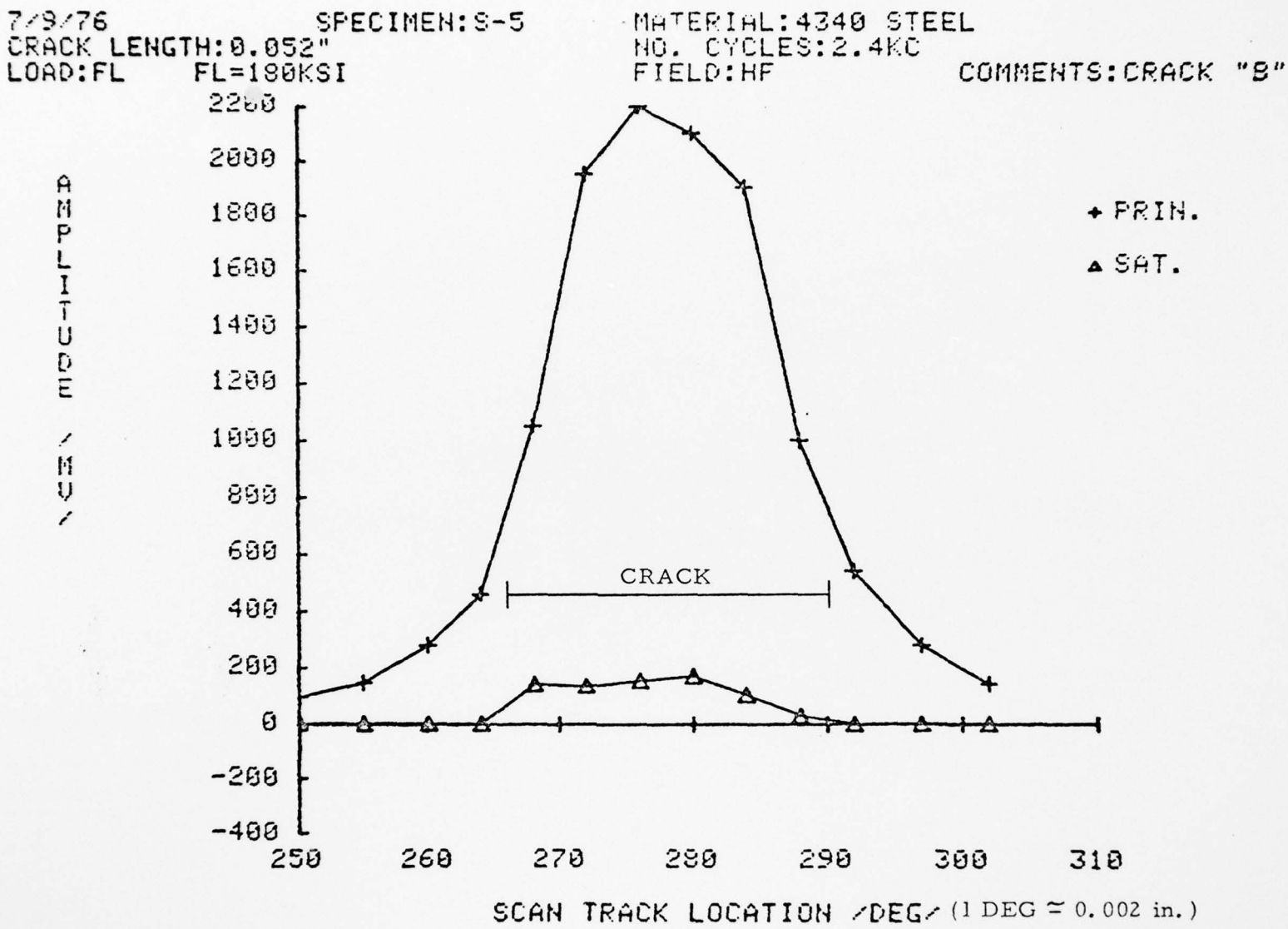

FIGURE 2. MAGNETIC PERTURBATION SIGNAL AMPLITUDE VERSUS LOCATION ALONG A FATIGUE CRACK.

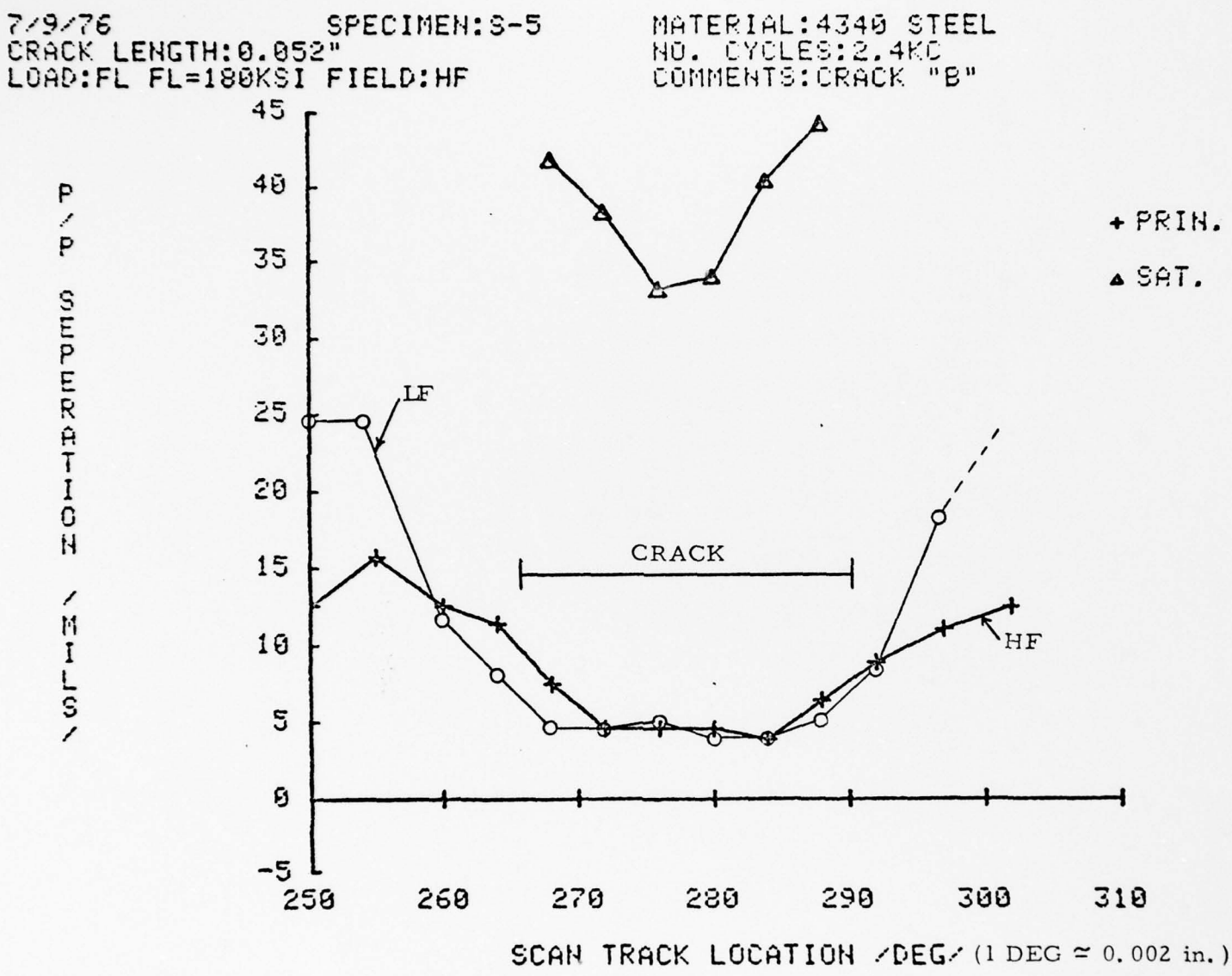

FIGURE 3. MAGNETIC PERTURBATION SIGNAL PEAK SEPARATION VERSUS LOCATION ALONG A CRACK INTERFACE.

1. Once the crack is opened by an applied load, the magnetic perturbation signal amplitude at the center of the crack is linearly related to the crack opening displacement, COD. Since magnetic field analysis[2] predicts that the magnetic perturbation signal amplitude is a linearly increasing function of volume, these results indicate that the volume between the crack interfaces is a linear function of COD.

2. Within limits of the experimental measurements, the magnetic perturbation signal peak separation does not change as the applied stress is changed from zero to 180 ksi, despite the fact that the magnetic perturbation signal amplitude increases by a factor greater than nine.

3. Previous results have indicated an approximately linear relationship between peak separation and the distance from the flaw centroid to the surface[3]. Furthermore, recent results indicate that the peak separation increases with fatigue crack length and is approximately equal to 1/3 the depth[1]. From the foregoing we are suggesting a "hinge" model for the opening of small surface entering fatigue cracks. If the crack opens at the middle, in response to applied external force as though the adjacent crack surfaces are hinged at the bottom, the experimental results are consistent; namely, the signal amplitude increases linearly with volume of the triangular opening and the peak separation is constant since the centroid is fixed. If the crack opens as a wedge with the apex increasing with opening, the volume would increase linearly with the triangular opening but the centroid would also move further from the base and the peak separation should increase - which is not the case.

4. The peak-to-peak separation of both the principal and satellite components is less at the interior regions of the crack than at the tips. (See Figure 3). This result is observed consistently for all crack lengths and applied loads investigated. Although no detailed explanation has been developed at this time, the results suggest that the peak separation may be related to the stressed zones around the fatigue crack. Analytical efforts utilizing the magneto-mechanical properties of the material are underway to explore this possible relationship.

5. For low magnetic fields, the variation in the signal peak-to-peak separation from the interior regions of the crack to the tip is greater than for the high field case as shown in Figure 3.

Efforts are under way to develop analytical models for explaining the behavior of the magnetic perturbation results in terms of the magneto-mechanical interactions in the fatigue crack region. In addition, experiments are planned to apply the magnetic perturbation technique to the investigation of fatigue cracks in other types of steel materials such as the AF 1410 steel described in the next section.

B. AF 1410 Steel Specimens

Rod-shaped fatigue specimens of AF 1410 steel are currently being prepared using material obtained from General Dynamics Convair Aerospace Division in Fort Worth. Heat treatment, putting the material into the solution-treated and aged condition, was performed by U. S. Steel. The heat-treat schedule was as follows:

Initial austenizing	1650°F for 60 minutes
Final austenizing	1500°F for 60 minutes
Aging	950°F for 8 hours

The material was water quenched after each heat treatment. Composition in weight percent as given by U. S. Steel is:

C	0.12	Mo	0.99
Mn	0.13	Co	7.76
P	0.007	Ti	0.01
S	0.003	Al	0.017
Si	0.07	N	75 PPM
Ni	9.93	O	25 PPM
Cr	2.00		

The average mechanical properties of the material as reported by General Dynamics for plate specimens is[4]:

Ultimate tensile strength	196,000 psi
0.2% tensile yield strength	183,600 psi
% Elongation	18.0
% Reduction in area	73.8

Hardness readings were made at SwRI on the machined fatigue specimens prior to finish grinding. These indicate a Rockwell hardness of approximately 43 Rc.

Since the AF 1410 material is electro-vacuum processed, it is anticipated that a large number of stress cycles will be necessary to generate fatigue cracks. Therefore, an automatic monitoring capability is being added to the stress-cycling machine to alleviate the need for constant manual monitoring of the specimen. This will permit operation 24 hours each day. The primary purpose of the automated system at this time is to monitor the outputs of ultrasonic surface wave transducers mounted on a fatigue test specimen and to automatically stop the fatigue testing machine if certain signatures appear in the transducer output signals.

A block diagram of the system is shown in Figure 4. Ultrasonic transducers mounted on fatigue test specimens communicate with a Sperry Reflectoscope by way of a coaxial relay switch which sequentially selects and interrogates each of six 10 MHz surface wave transducers bonded to flats on the specimen. Control of the coaxial relay switch and the fatigue machine motor is performed by means of a microcomputer system. Ultrasonic echoes reflecting from fatigue cracks and exceeding a preset threshold level in the Reflectoscope will send an alarm signal to the microcomputer. Recognition by the microcomputer of fatigue crack initiation results in a command to shut down the fatigue testing machine. Pertinent information such as cycle count at alarm and the transducer initiating the alarm can be printed out on a teletype for further inspection. Extension of the system to signal processing of the ultrasonic signals, or of other information such as magnetic perturbation signals or Barkhausen noise signals, can be performed in the future by integrating the system with either a Tektronix Graphic Computing System or a Hewlett-Packard Minicomputer which can be made available for this purpose.

C. Barkhausen Noise Analysis

As has been previously shown, the Barkhausen noise analysis method can be used to measure both residual and applied stress[5]. To obtain adequate resolution for measuring the stress fields in the vicinity of small fatigue cracks, it was necessary to fabricate a smaller size Barkhausen probe than had heretofore been available. For the work reported here, a Barkhausen sensing coil 0.010-inch wide x 0.010-inch high x 0.015-inch long was fabricated and mounted in a micrometer adjustment fixture on the stress-cycling machine. This arrangement facilitates very precise location of the Barkhausen probe relative to the fatigue cracks. Because of the small size of the Barkhausen probe, a very sensitive pulse preamplifier was required. The large magnetizing coil used for the magnetic perturbation measurements was also utilized to cyclically magnetize the specimens for Barkhausen measurements. For most of the work, a magnetic cycling frequency of 3 Hz was selected.

Barkhausen noise data were taken on an AISI 4340 steel specimen, S5, which previously had been cycled at a maximum stress of 180 ksi (0.2% tensile yield strength for this specimen = 183 ksi). This is the same specimen used for the magnetic perturbation investigations reported in Section A. Figure 5 shows the Barkhausen signal peak amplitude as a function of applied static stress for an uncracked region of the specimen and at the center of a 0.052-inch long crack. These data were taken near the center of the gage section of the specimen. Previous Barkhausen results obtained on cantilever bending specimens of AISI 4340 steel show that a plot of the Barkhausen signature versus both tensile and compressive applied

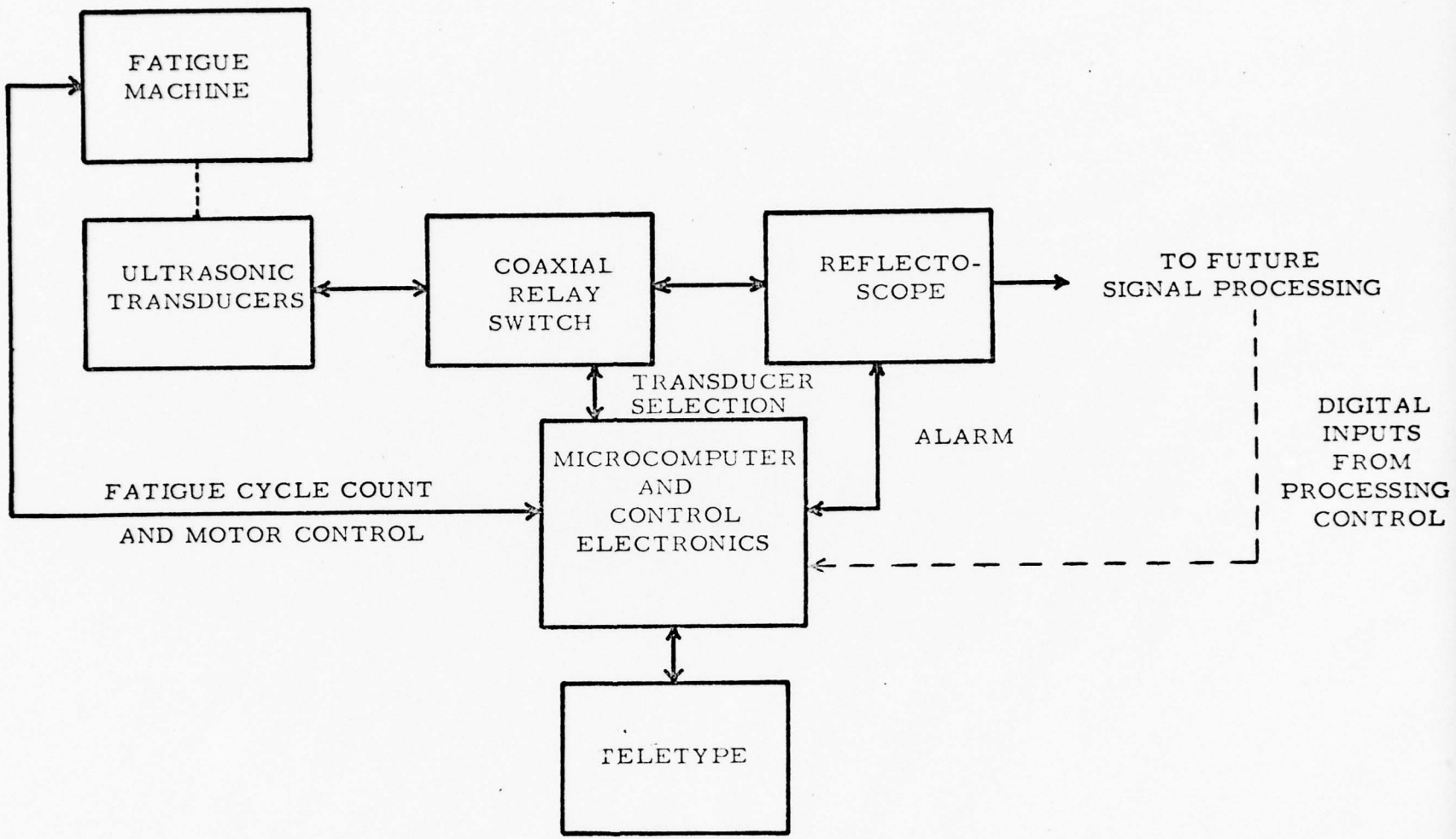

FIGURE 4. BLOCK DIAGRAM OF AUTOMATED CONTROL SYSTEM FOR STRESS-CYCLING MACHINE.

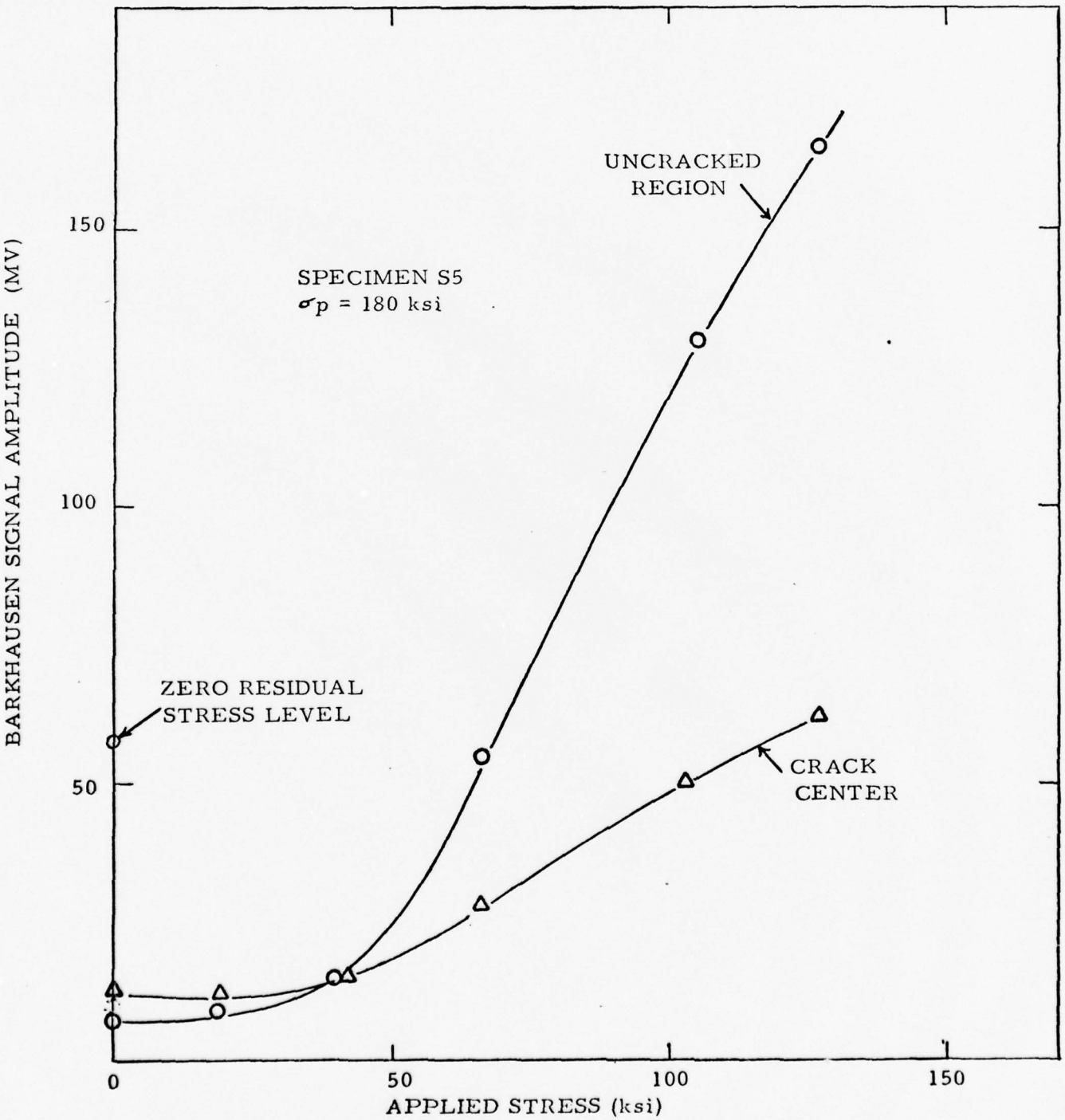

FIGURE 5. BARKHAUSEN SIGNAL AMPLITUDE VERSUS APPLIED STATIC TENSILE STRESS FOR SPECIMEN S5.

stress produces an S-shaped curve when the residual stresses are near zero[6,7]. Data obtained on an AISI 4340 rod-type fatigue specimen which was subjected to applied tensile stress are shown in Figure 6 (compressive stress could not be applied without buckling the specimen). These results are for specimen S30 which had been subjected to peak stresses of only 130 ksi, well below the yield stress of 183 ksi. Note that the Barkhausen signal increases with increasing tensile stress, reaches a maximum at approximately 30% of the yield stress, and then slightly decreases with the application of additional stress. Referring back to Figure 5, the fact that the Barkhausen data do not show a flattening at the upper end for stresses up to 112 ksi, but do show significant flattening at the low end, even up to applied stress of 40 ksi, indicate that the region of the specimen near the center is in a state of compression. The fact that the specimen had been cycled at a stress near yield, and that the Barkhausen data were taken in the narrow part of the specimen where the section stress would be the greatest, seems to imply that a state of residual compression could likely exist.

To establish the Barkhausen signal amplitude corresponding to zero stress and to corroborate the above analysis of the data presented in Figure 5, a Barkhausen measurement with no applied stress was made further up on Specimen S5, well out of the gage section, where the residual stress should be near zero. This measurement yielded a Barkhausen signal amplitude of approximately 60 mV. This level is indicated in Figure 5. A comparable Barkhausen signal amplitude was obtained from another specimen of AISI 4340 steel which had been cycled at a much lower stress level, namely, 130 ksi, and therefore should be in essentially a zero residual stress condition. Thus 60 mV should be the zero residual stress Barkhausen signal amplitude level for these specimens.

Extensive Barkhausen measurements were made on Specimen S5 in the vicinity of three fatigue cracks. Approximately 400 Barkhausen signals were obtained on a square matrix grid pattern based on 0.010 inch centers. One approach to analyzing these data is to plot constant Barkhausen contours in an effort to appraise the surface stress distribution. Preliminary analysis indicates significant variations in the contours in the vicinity of the fatigue cracks, but further fracture mechanics analysis will be necessary to guide interpretation of the Barkhausen readings in terms of stress distributions around fatigue cracks. Additional Barkhausen data will be taken on specimens cycled at other stress levels in order to relate the results to variations in the plastic zone size. It is expected that these results will help in the analysis and interpretation of magnetic perturbation signatures obtained from fatigue cracks as well as in the application of fracture mechanics to a determination of crack criticality.

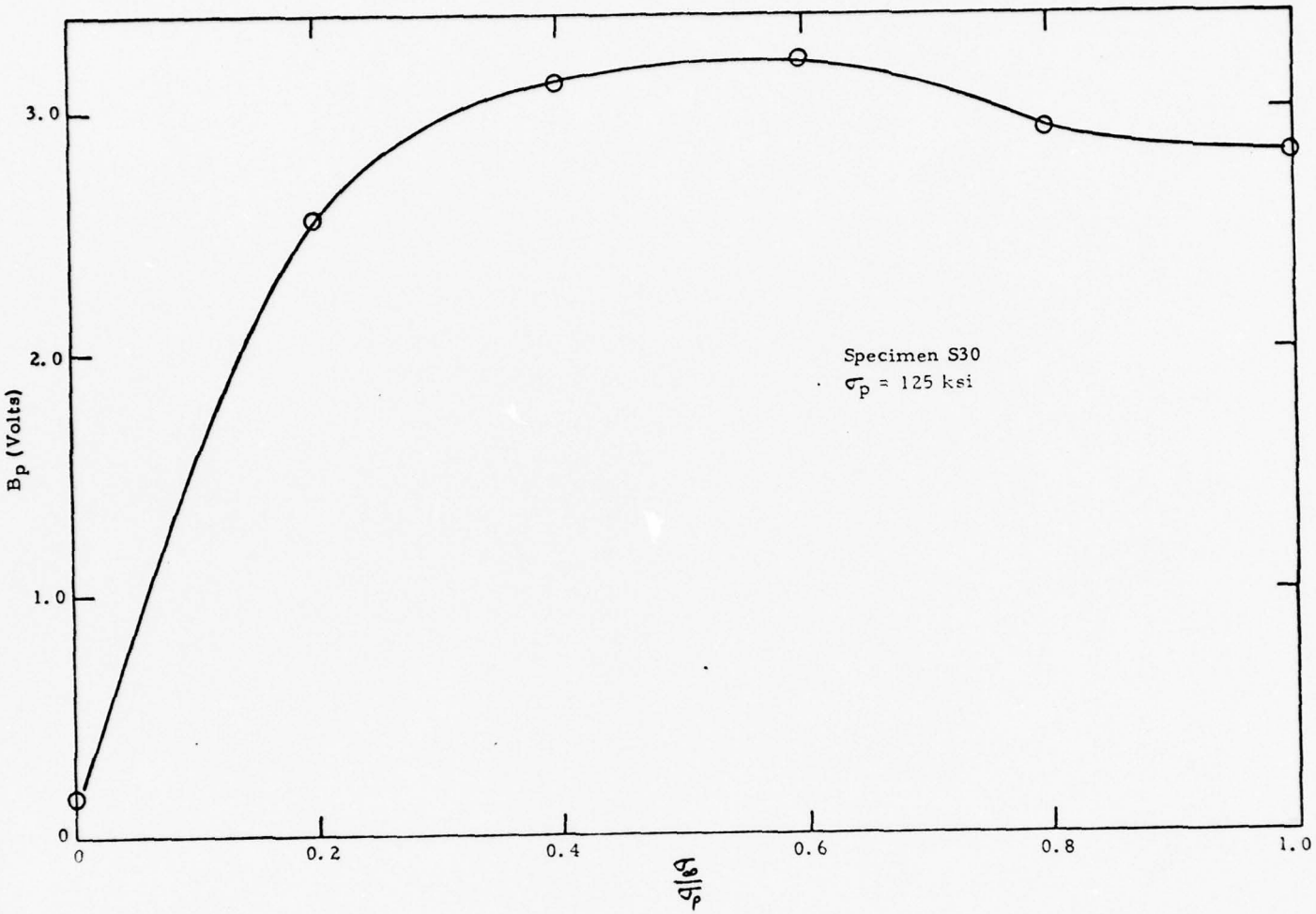

FIGURE 6. BARKHAUSEN NOISE SIGNAL AMPLITUDE VERSUS APPLIED STATIC TENSILE STRESS

D. AC Four-Contact Electric Probe Measurements

One of the crack parameters on which quantitative information is needed in order to apply fracture mechanics to the analysis of fatigue cracks is the crack depth. Previous work on relatively large fatigue cracks in plate specimens has shown that an NDE technique capable of giving signals quantitatively correlated with the crack depth is the AC electric potential method using four-contact probes[8]. In this method two outer electrical contacts inject current into the specimen and two inner contacts sense the electric potential. If a crack is present between the inner contacts the potential is higher than that for uncracked material and the potential difference is related to the crack depth. The application of this method is described in more detail in the Appendix.

The precision of the measurement depends on the relationship between the crack depth and the probe contact spacing which should be comparable to the crack depths of interest. For this condition, the response of the probe can be analyzed theoretically for two ranges of crack lengths:[9]

1. If the surface length of the crack, L, is long compared to the contact spacing, A, then the measured voltage is given by the equation

$$V \simeq V_o (1 + CD) \tag{1}$$

where V_o is the potential between the voltage contacts for uncracked material, D is the crack depth, and C is a calibration constant.

2. If on the other hand, the crack length is small compared to the contact spacing, A, then the measured voltage also depends on the crack length. In this case, the lower order of approximation introduces a crack effect proportional to the product of the crack length and depth. For a half-penny shaped crack the measured probe voltage is given by the equation

$$V \simeq V_o (1 + K^2 D^2) \tag{2}$$

where K is a calibration constant.

For measurements on fatigue cracks with lengths in the range of 0.010 inch to 0.050 inch, it was necessary to design and fabricate a miniature four-contact probe having minimal contact spacing. It was found convenient to do this using commercially available spring-loaded contacts, in which a fine tungsten wire slides inside a flexible guide tube. The contact spacing achievable is governed by the guide tube diameter which is 0.006 inch; the diameter of the tungsten contact is 0.003 inch. Four of these flexible

contacts arranged linearly on 0.010 inch centers were encapsulated into a plastic block. The completed four-contact probe was mounted in a micrometer adjustment fixture on the stress-cycling machine so that the vertical position of the probe could be very accurately located relative to the fatigue cracks in the specimens of interest.

In order to obtain quantitative information on the crack depth, it is necessary to first calibrate the four-contact probe on defects of known dimensions in the material of interest. In the work reported here, four-contact probe measurements were performed on specimens of Ti-6Al-4V alloy which were also used in the electric current injection investigations to be discussed in the next section. To calibrate the probe before applying it to the measurement of fatigue cracks, a block of Ti-6Al-4V was used into which a series of EDM notches were machined comparable in depth and length with the fatigue cracks of interest, that is, in the range of 0.010 inch to 0.050 inch. A tungsten EDM tool was used which had been etched to a semi-circular shape to simulate a half-penny shaped crack. The width of the notches was approximately 0.005 inch; the length, depth, and width of each notch was determined optically with a measuring microscope.

The four-contact electric probe data from EDM notches plotted against notch depth are shown in Figure 7. According to the theoretical analysis discussed previously, for notch depths less than the probe contact spacing of approximately 0.010 inch, the measured voltage should depend on the notch depth according to the equation:

$$\left(\frac{V - V_o}{V_o}\right)^{1/2} = KD \qquad (3)$$

Examination of the top part of Figure 7 shows that the experimental data agree well with this dependence for notch depths up to approximately 0.012 inch with $K = 68.6$ in.$^{-1}$. For notch depths greater than 0.012 inch, the measured voltage is found to conform with the dependence

$$\frac{V - V_o}{V_o} = CD \qquad (4)$$

where $C = 52.0$ in.$^{-1}$, in agreement with the theoretical analysis. Thus, in general, the four-contact electric probe measurements on small machined notches in Ti-6Al-4V agree well with electric potential theory and should provide a means for determining the depth of fatigue cracks.

FIGURE 7. AC FOUR-CONTACT ELECTRIC PROBE VOLTAGE VERSUS EDM NOTCH DEPTH IN Ti-6Al-4V.

After calibrating the probe, AC four-contact probe measurements were made on a rod-shaped tensile specimen of Ti-6Al-4V in which a fatigue crack was generated and grown to approximately 0.050 inch long with a maximum cyclic stress of 130 ksi. Stress cycling was interrupted at various crack lengths and four-contact electric probe measurements were made at a number of locations along the crack interface. Typical data obtained are shown in Figure 8 for crack lengths of 0.020 inch and 0.040 inch. Usually, the measurements were made with zero static stress applied to the specimen. No changes in the four-contact probe measurements were observed when stress was applied to the specimen indicating that tight closure does not significantly affect the electric probe measurement, in agreement with previous work[8].

The four-contact electric probe data from the fatigue crack were used in conjunction with the calibration constants determined from EDM notches to compute the fatigue crack depth. These results compared to the crack depth according to a half-penny assumption are shown in Table I.

TABLE I

Crack Length (in.)	$(V-V_o)/V_o$	Calibration Constant ($in.^{-1}$)	Computed Depth (in.)	Depth by Half-Penny Approximation (in.)
0.010	0.13	68.6	0.005	0.005
0.020	0.41	68.6	0.009	0.010
0.030	0.72	52.9	0.014	0.015
0.040	0.95	52.0	0.018	0.020
0.050	0.15	52.0	0.022	0.025

As can be seen, the agreement between the crack depth measured with the four-contact probe and the half-penny assumption is very good and indicates that the AC four-contact electric potential method can be satisfactorily used to obtain fatigue crack depth using calibration constants from machined notches. The slight discrepancies in the crack depth results noted in Table I are probably associated with the approximations inherent in the theoretical analysis used to compute the crack depths. However, for most purposes, the accuracy of the measurement should be adequate.

Additional work is required to determine the general reliability of the method and the levels of confidence for fatigue crack determination. Also, the applicability of the method to other types of materials, especially high strength steels needs to be explored. In general, for the laboratory determination of fatigue crack depth, the AC four-contact electric probe method appears to be very promising.

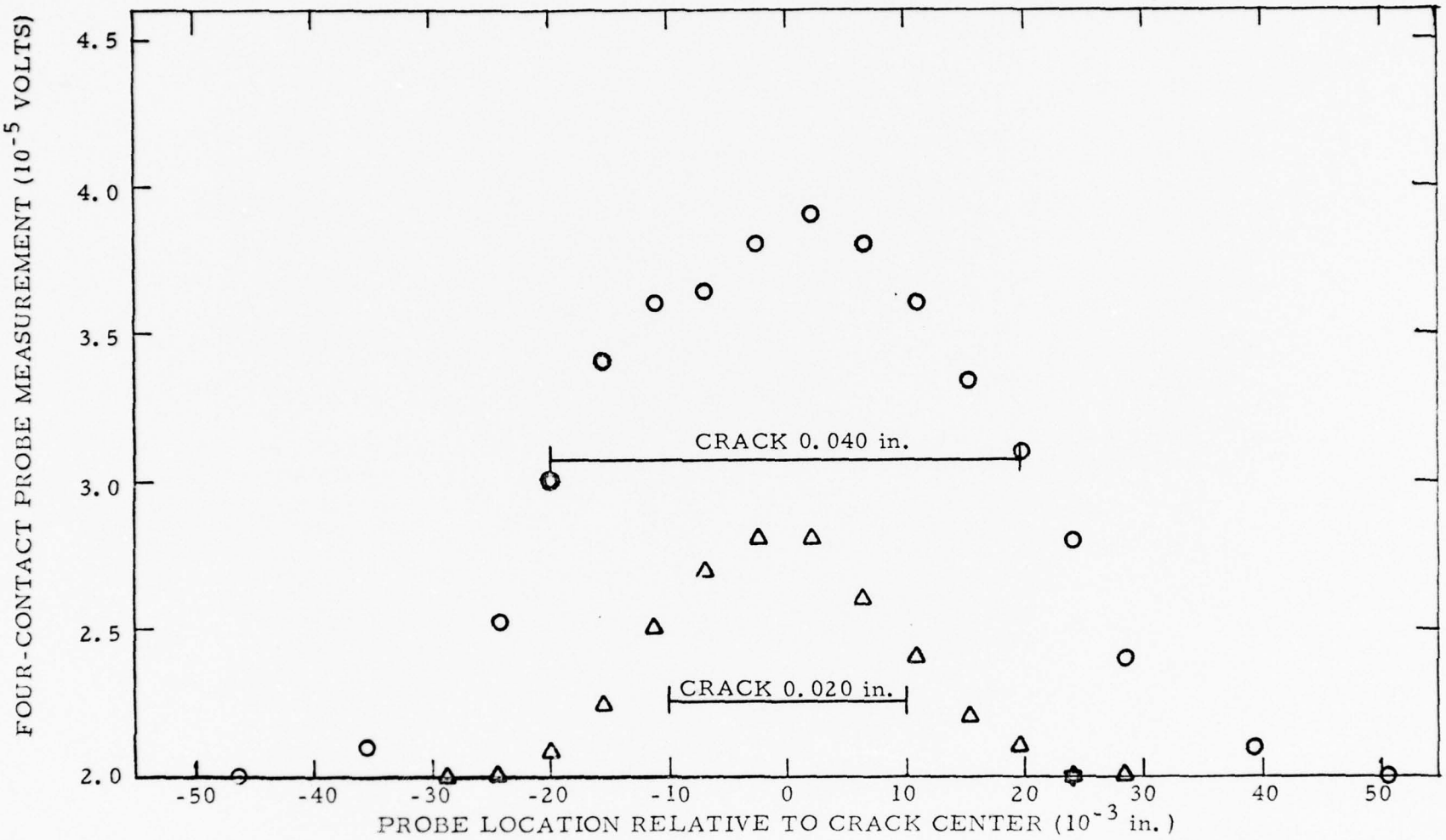

FIGURE 8. AC FOUR-CONTACT ELECTRIC PROBE MEASUREMENTS ALONG THE INTERFACES OF TWO FATIGUE CRACKS IN Ti-6Al-4V.

E. Electric Current Injection

Electric current injection data have been obtained on a specimen of Ti-6Al-4V alloy in which a fatigue crack was generated and grown to a length of 0.050 inch. This was the same specimen used for the AC four-contact electric probe measurements discussed in the previous section. For the electric current injection investigations, a current of approximately 1.7 amps RMS was induced in the specimen at a frequency of 10 kHz. A small inductive pickup coil was used to detect the perturbations in the magnetic field associated with the current flow around the fatigue crack. The probe was mechanically scanned in the direction of the specimen axis, perpendicular to the crack interface. Synchronous detection at the drive frequency of 10 kHz was used to increase the sensitivity and discriminate against incoherent noise.

Stress cycling was interrupted at various crack lengths within the range of 0.010 inch to 0.050 inch. At each crack length, electric current injection signals were obtained along 20 scan tracks perpendicular to the crack interface from approximately 1/2 the crack length beyond one crack tip to a comparable distance beyond the other crack tip. The shape of the detected signal typically varied with location along the crack interface as shown in Figure 9. As is seen in the Figure, the fatigue crack produces signals which reverse polarity as the crack interface is traversed, going through a null at the center of the crack. Figure 10 is a graph of the variation in the amplitude of the major peak relative to location along the interface of a 0.050-inch long crack. In general, applied stress has little effect on the observed signals. Analysis of the data shows that the maximum peak-to-peak signal amplitude is related to the crack interface area as shown in Figure 11. Similar correlations between signal amplitude and defect area have been obtained for other specimen geometries[10]. The crack depth used in computing the crack interface area indicated in Figure 11 was obtained by the four-contact electric probe measurements as described in the previous section.

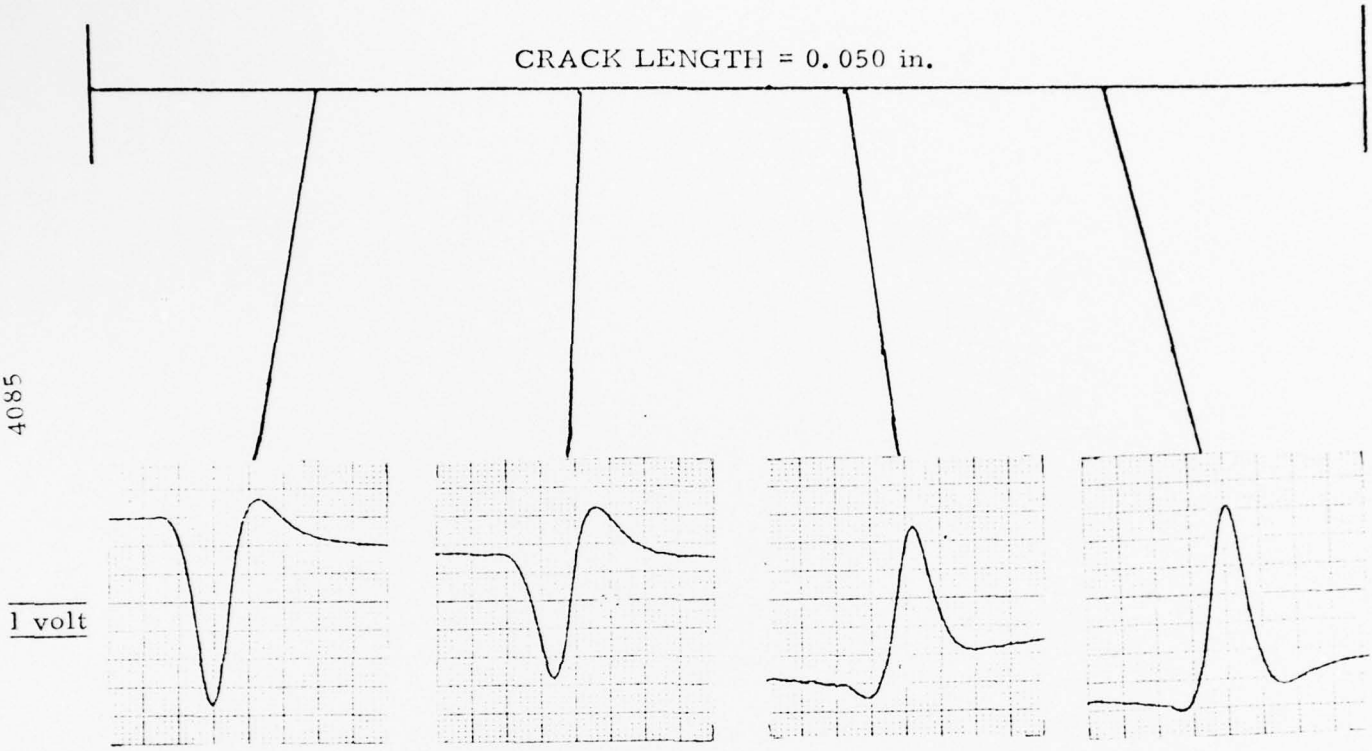

FIGURE 9. VARIATION OF ELECTRIC CURRENT INJECTION SIGNAL ALONG A CRACK INTERFACE IN Ti-6Al-4V.

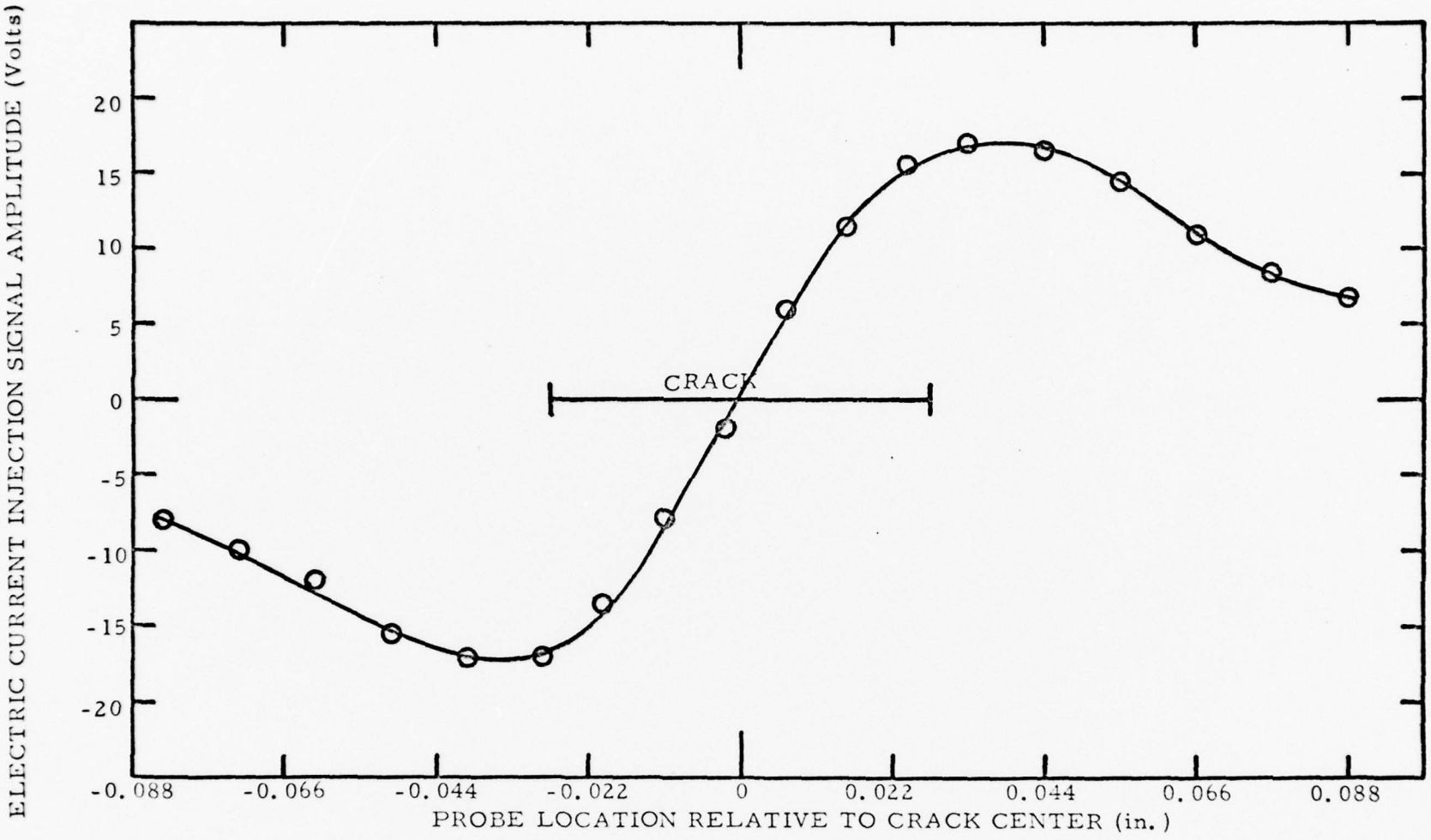

FIGURE 10. ELECTRIC CURRENT INJECTION SIGNAL AMPLITUDE VERSUS LOCATION ALONG A FATIGUE CRACK INTERFACE IN Ti-6Al-4V.

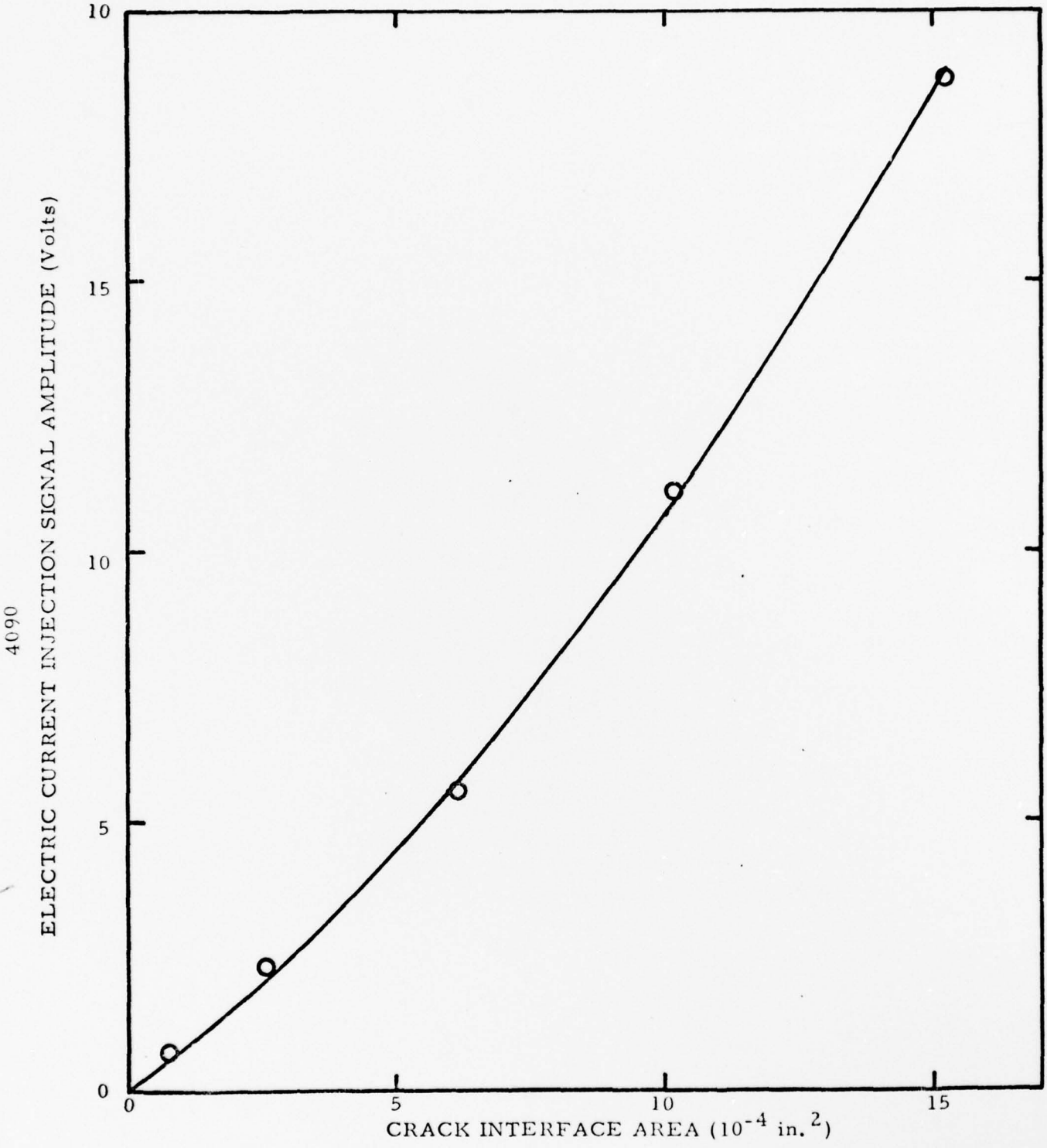

4090

FIGURE 11. ELECTRIC CURRENT INJECTION SIGNAL AMPLITUDE VERSUS CRACK INTERFACE AREA IN Ti-6Al-4V.

III. CLOSING REMARKS

Work is continuing in both the experimental and analytical areas. Six rod-type fatigue specimens of AF 1410 steel are being fabricated; machining has been completed and the specimens are currently being subjected to a finish-grind procedure. It is anticipated that one or more of these specimens will be stress-cycled within the present program using the automatic fatigue-crack-monitoring facility. Fatigue cracks will be grown to various lengths up to 0.050 inch long and investigated using magnetic perturbation, ultrasonics and Barkhausen noise analysis. These results will be compared to those obtained on AISI 4340 steel specimens and analyzed in terms of independently measured crack parameters. Fracture mechanics analysis will be used to interpret the NDE measurements and to analyze the fatigue crack initiation and growth characteristics in AF 1410.

Analytical work is continuing in efforts to interpret the various features of the NDE measurements in terms of the crack parameters needed for determination of crack criticality by fracture mechanics analysis. Both the mechanical characteristics of the crack region, and the magnetic characteristics in the case of steels, are being considered in order to obtain realistic models for interpreting the quantitative functional relationship between the various NDE signatures and the pertinent crack parameters, such as length, depth, COD, crack interface area, crack opening configuration, and plastic zones.

Results of these efforts are expected to lead to the ability to characterize fatigue cracks quantitatively so that in conjunction with fracture mechanics analysis, a scientific basis will be available for assessing the criticality of a detected crack. This ability should be of importance to the Air Force in relation to design criteria used for structural configurations as well as provide a better basis for maintenance.

IV. PUBLICATIONS

Results of work conducted during the past year under AFOSR Contract No. F44620-75-C-0042 were included in an invited presentation made at the Sagamore Research Conference in August 1976:

> "Advanced Quantitative Magnetic Nondestructive Evaluation Methods - Theory and Experiment", J. R. Barton, F. N. Kusenberger, R. E. Beissner, and G. A. Matzkanin, Twenty-Third Sagamore Army Materials Conference, Raquette Lake, New York, August 24-27, 1976. Proceedings are in the process of being published.

V. REFERENCES

1. Kusenberger, F. N., Matzkanin, G. A., Barton, J. R., and Francis, P. H., "Nondestructive Evaluation of Metal Fatigue," AFOSR-TR-76-0384, March 1976.

2. Barton, J. R., Kusenberger, F. N., Beissner, R. E., and Matzkanin, G. A., "Advanced Quantitative Magnetic Nondestructive Evaluation Methods - Theory and Experiment", Twenty-Third Sagamore Army Materials Research Conference, Aug. 24-27, 1976. Proceedings to be published.

3. Barton, J. R., "Quantitative Correlation Between Magnetic Perturbation Signatures and Inclusions," in Bearing Steels. The Rating of Nonmetallic Inclusions, STP 575, pp. 189-213, May 1975.

4. Jones, R. L. and Margolis, W. S., "Advanced Metallic Air Vehicle Structure Program," Material Property Data Test Report - Credible Option, Contract AF33615-73-C-3001, October, 1975. (Unpublished).

5. Donaldson, W. L. and Pasley, R. L., "A New Method of Nondestructive Stress Measurements," Proceedings of the Sixth Symposium on Nondestructive Evaluation of Aerospace and Weapons Systems Components and Materials, Western Periodicals Co., Los Angeles, 1967, pp. 563-575.

6. Birdwell, J. A. and Barton, J. R., "Development and Application of Barkhausen Instrumentation Concepts for Measuring Stress in Ferromagnetic Steels," Final Report, Contract No. N00156-71-C-0362, Naval Air Engineering Center, Philadelphia, Pennsylvania, September, 1971. Unpublished.

7. Barton, J. R., and Kusenberger, F. N., "Residual Stresses in Gas Turbine Engine Components from Barkhausen Noise Analysis," Paper 74-GT-51, ASME Gas Turbine Conference, Zurich, Switzerland, April 1974.

8. Birchak, J. R., "AC Four-Contact Electric Probe for Determining Fatigue Crack Depths," Proc. 10th Symposium on NDE, San Antonio, April 23-25, 1975, pp. 19-29.

9. Gille, G., "The Electrical Potential Method and its Application to Nondestructive Testing," Nondestructive Testing (London), 4, pp. 36-44, Feb. 1971.

10. Baker, J. H., Kusenberger, F. N., and Perry, W. D., "Feasibility Study for Current Injection Inspection of Aluminum and Titanium Tubes", SwRI Final Report, Purchase Order NA 430672, The Boeing Company Vertol Division, Mar. 1970. Unpublished

APPENDIX

Specimens

Tensile fatigue specimens of AISI 4340 steel were rough-machined to shape from one-inch diameter bar stock which had been austenitized at 1525°F for two hours, oil-quenched, and air tempered for four hours at 975°F. Hardness readings resulting from this heat treatment were in the range 35-37 Rc. Final machining (grinding) and polishing operations followed. All specimens, except for those used in replication microscopy studies, were hand polished using successively finer carborundum and emery papers, ending with No. 4/0, followed by final polishing with 0.3 μ alumina. The specimen configuration is shown in Figure 12.

Titanium, Ti-6Al-4V, specimens were rough-machined to shape from normal 1-inch-diameter mill-annealed certified material and then stress-relieve-annealed at 1100°F for 1 hour and air-cooled. Final machining and polishing operations on the titanium specimens were carried out similar to those used for the steel specimen. The finished specimen surface was similar in appearance to that of the steel specimen.

Table I summarizes the mechanical properties of the two types of specimen materials.

TABLE I

MECHANICAL PROPERTIES OF SPECIMEN MATERIALS

	AISI 4340	Ti-6Al-4V
Ultimate tensile strength	194, 150 psi	142, 830 psi
0.2% tensile yield strength	182, 550 psi	134, 500 psi
Elastic modulus	$35. \times 10^6$ psi	
% elongation	14.3	16.7
% reduction in area	48.5	41.5

The 4340 steel properties reported in Table I are the average results from two specimen tests and the titanium properties are those obtained from the mill certification of test.

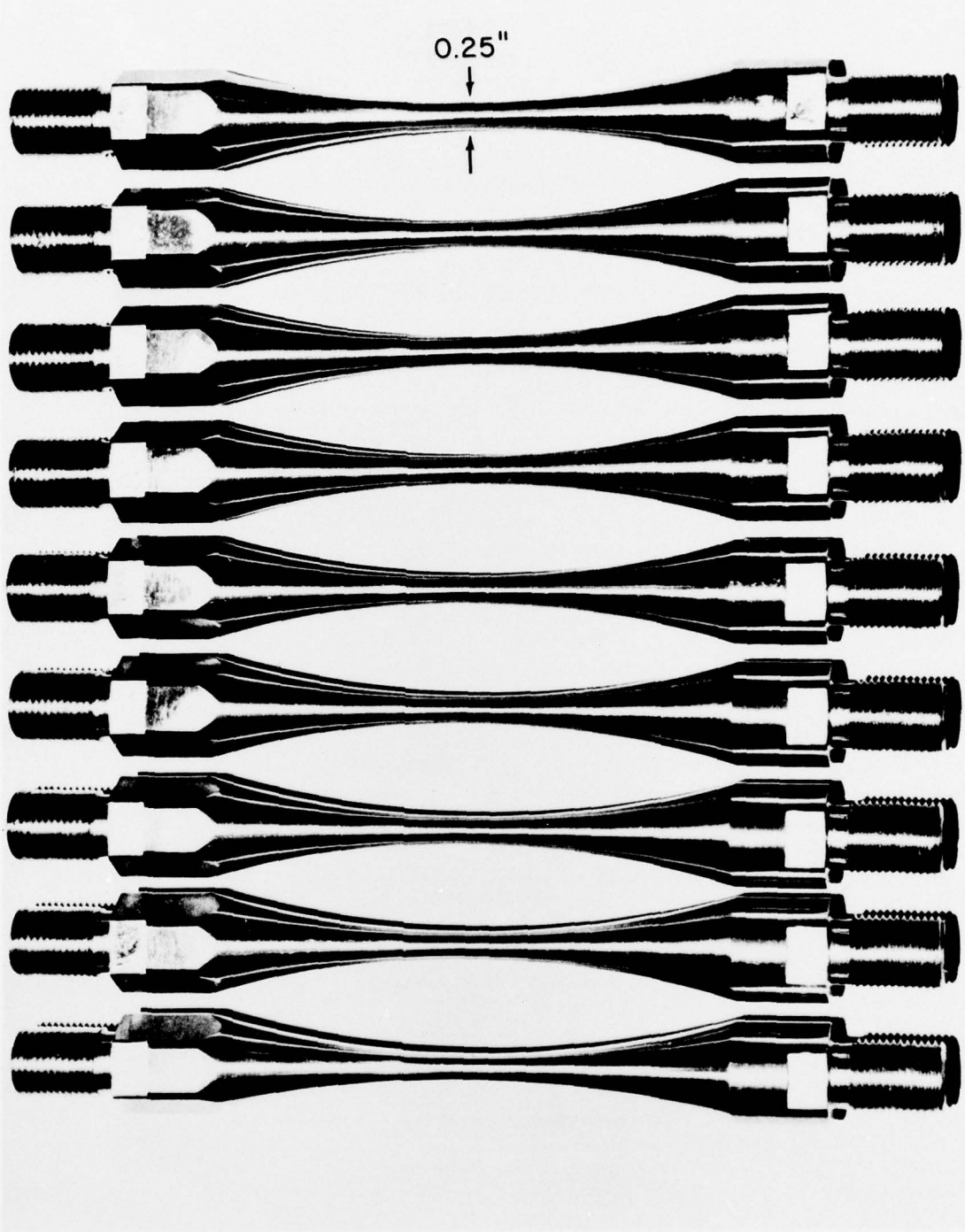

FIGURE 12. PHOTOGRAPH SHOWING SEVERAL TYPICAL AISI 4340 STEEL TEST SPECIMENS

Experimental Procedure

The specimens were stress cycled in uniaxial tension in the laboratory ambient air environment using the facility shown in Figure 13. A close-up view of the test specimen area encircled in Figure 13 is presented in Figure 14. Components of some of the NDE instrumentation are also pointed out in Figures 13 and 14. The specimens were cycled using a zero-to-peak stress of the desired value with a stress ratio R = 0, and were continuously monitored with ultrasonic surface wave instrumentation until the initiation of a fatigue crack was noted. The largest crack as determined with an optical microscope was chosen for further investigation. After growing the crack to the desired length, the stress-cycling machine was stopped and measurements were made at various values of applied static stress.

In addition to the various NDE measurements, data of the following types were obtained for each of the crack-load conditions:

a. Crack lengths were measured at the surface using a bifilar micrometer eyepiece on a microscope.

b. Surface photomicrography (100X magnification) was performed to record the crack topology.

c. Ultrasonic surface wave pulse-echo signals were obtained from six transducers bonded to the specimen.

d. Replicas were made for determination of the crack opening displacement with the scanning electron microscope.

Experimental Methods

In the magnetic perturbation method, an electromagnet is used to magnetize the specimen while the surface of the specimen is scanned with a small magnetometer to detect minute perturbations in the magnetic leakage field. The perturbations can be caused by defects in the specimen such as inclusions, voids, cracks, localized residual stresses, chemical segregation, etc. The method is schematically illustrated in Figure 15 for the case of an inclusion. In the present program, magnetic perturbation inspection of the specimen was accomplished by scanning the surface of the specimen with a Hall-effect transducer that transforms the magnetic perturbations into electrical signals which are then recorded. Recent improvements in Hall probe design have made it possible to resolve heretofore unobservable changes in magnetic signal characteristics associated with fatigue crack development in the vicinity of tiny material inclusions. By means of a probe scanning mechanism the Hall probe was made to traverse a path along the specimen axis (perpendicular to the crack interface). Typical signatures are shown in Figure 16.

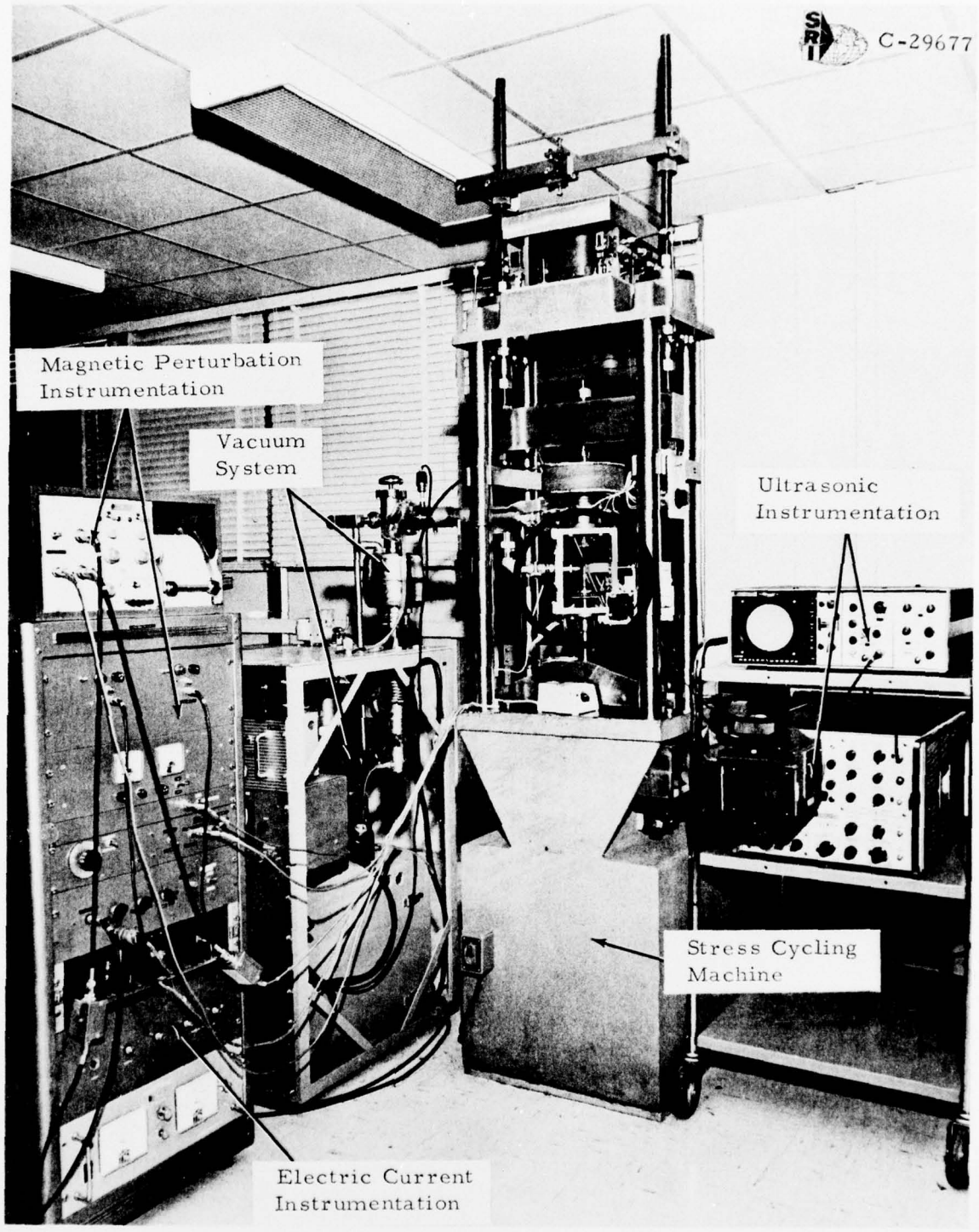

FIGURE 13. OVERALL VIEW OF NONDESTRUCTIVE FATIGUE EVALUATION FACILITY

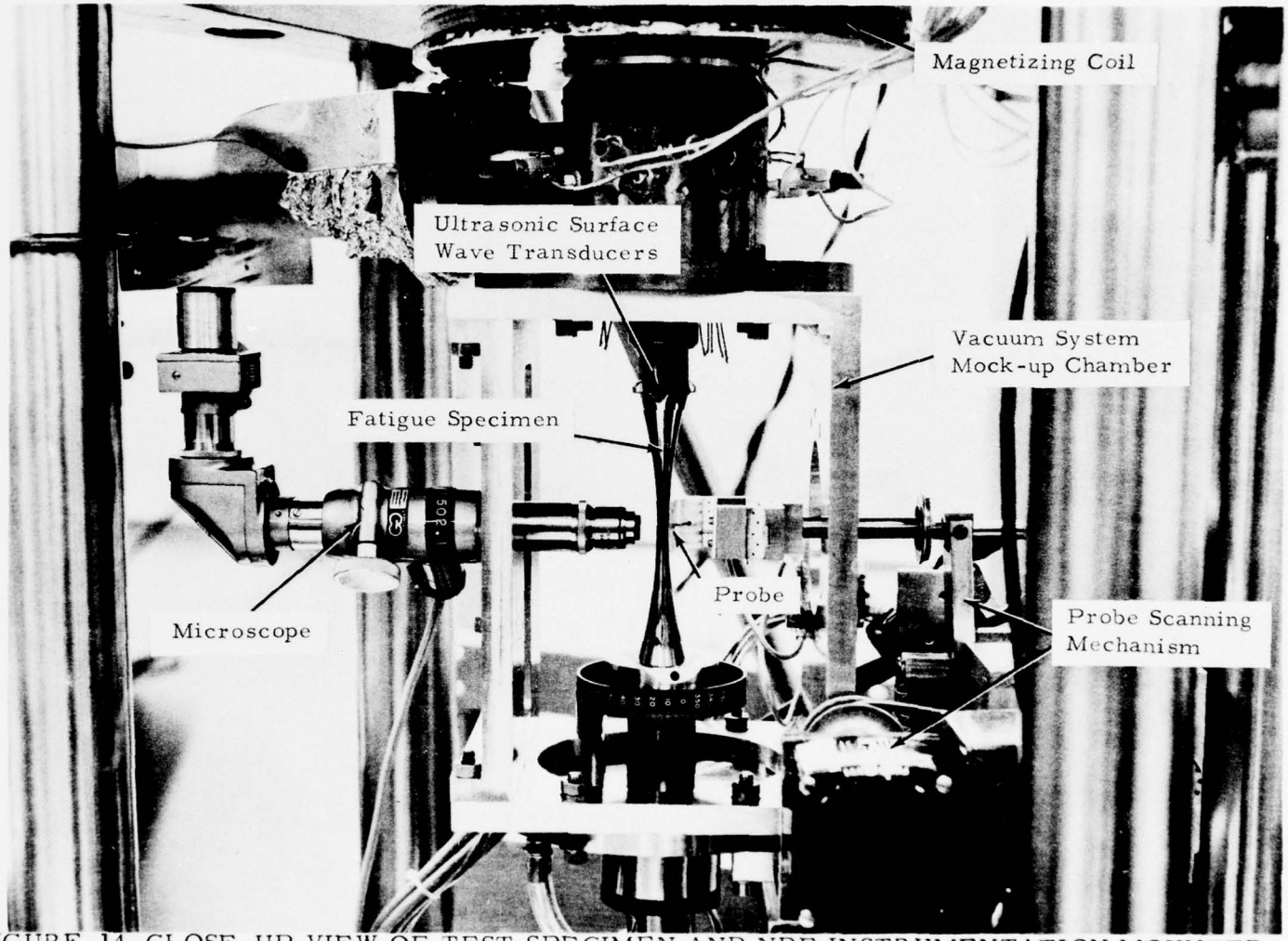

FIGURE 14. CLOSE-UP VIEW OF TEST SPECIMEN AND NDE INSTRUMENTATION MOUNTED IN FATIGUE TESTER

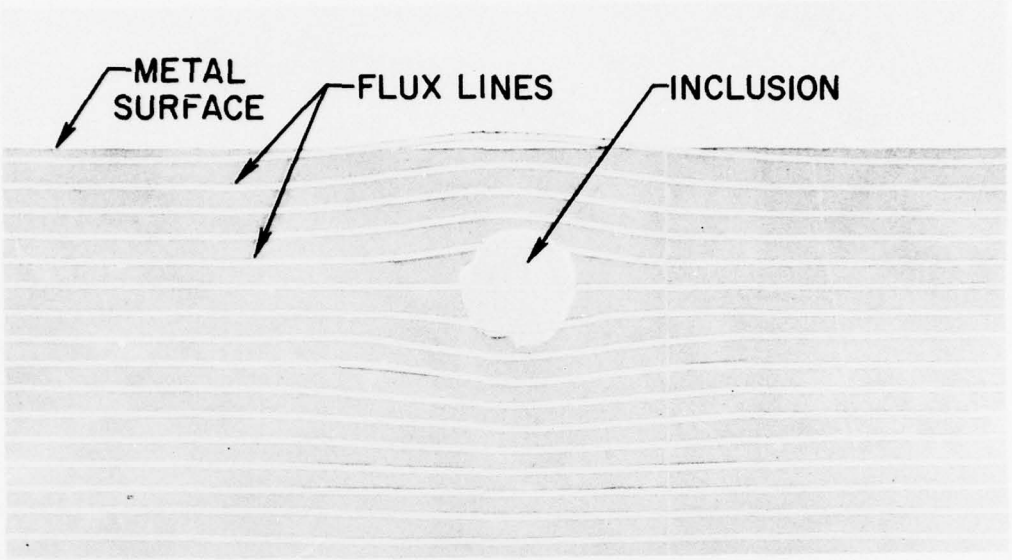

FIGURE 15. PERTURBATIONS IN MAGNETIC FLUX CAUSED BY INCLUSION IN FERROMAGNETIC MATERIAL.

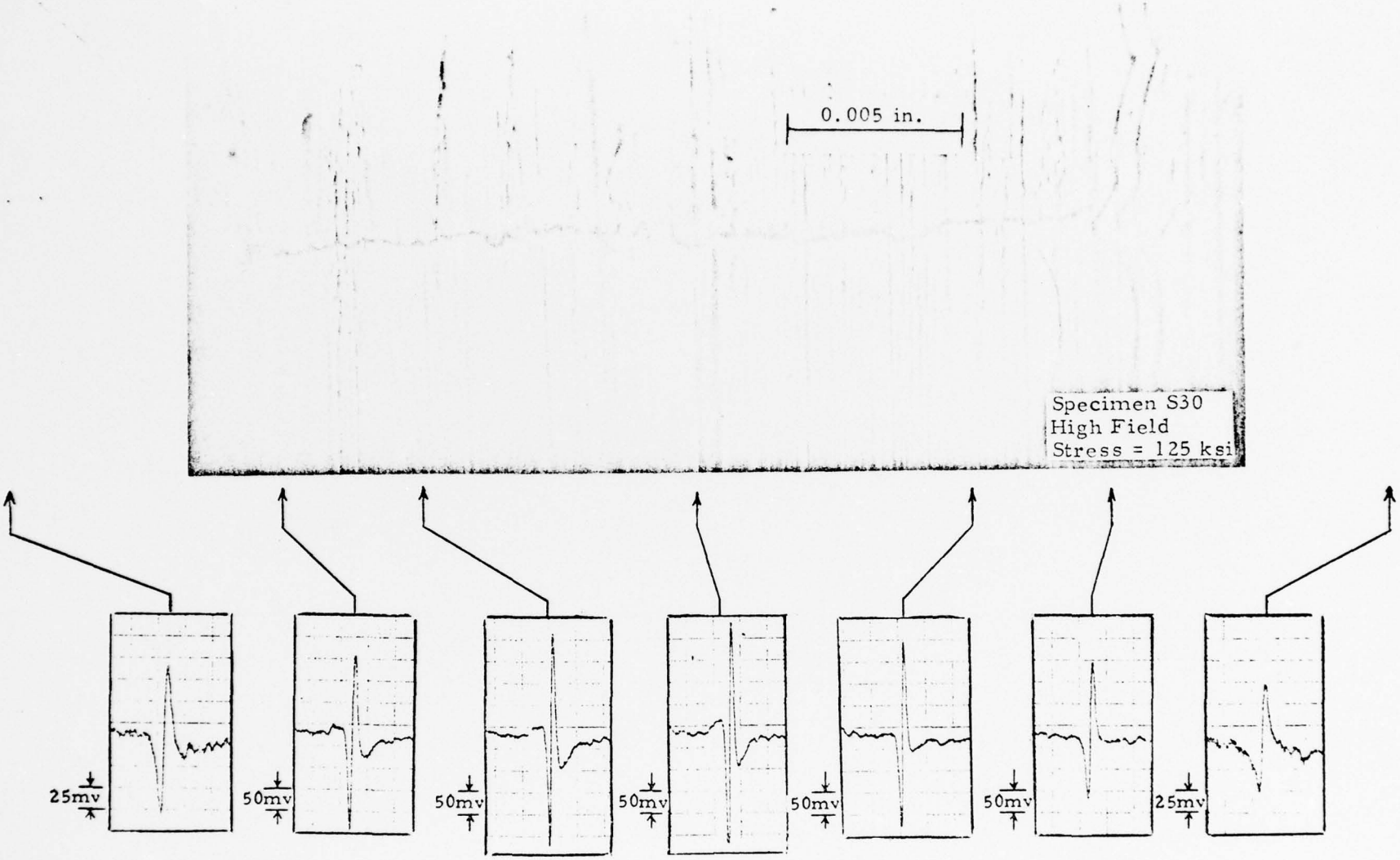

FIGURE 16. PHOTOMICROGRAPH SHOWING A FATIGUE CRACK WITH ASSOCIATED MAGNETIC RECORDS.

The Barkhausen noise analysis method involves application of a controlled magnetic field sequence to the specimen which causes a rearrangement of the magnetic domain structure. The domain rearrangements occur abruptly and the associated discrete changes in specimen magnetization induce voltage pulses in a detection coil placed in proximity to the specimen. This approach is illustrated schematically in Figure 17. The Barkhausen noise is strongly influenced by various parameters of the specimen, in particular the state of mechanical stress, and therefore it can be used to determine the residual stress around a fatigue crack. In experiments performed on fatigue specimens mounted in the stress-cycling machine, the controlled magnetic field sequence was applied with the same magnetizing coil used for the magnetic perturbation experiments. The Barkhausen probe was a small inductive coil which could be mounted on a micrometer adjustment fixture.

The electric current injection method for investigating fatigue cracks in nonferromagnetic metals is analogous to the magnetic perturbation method used for magnetic materials. Figure 18 is a schematic illustration of the method. A specimen is inspected utilizing this method by establishing a suitable current flow in the specimen and detecting deviations in this current flow caused by material inhomogeneities, such as inclusions, chemical segregations, cracks, etc. The deviations in current flow produce perturbances in the associated magnetic field and these are detected by a small noncontacting magnetometer probe scanned over the specimen surface. The signal output information from the probe is an electrical voltage and can be readily displayed on an oscilloscope or printed out on a strip chart recorder.

The AC Four-Contact Electric Probe method is an electrical potential approach whereby two outer electrical contacts inject current and two inner contacts sense the electric potential, as shown schematically in Figure 19a. The presence of a crack between the inner contacts causes a disruption of the electric potential due to the insulating barrier formed by the crack, as shown in Figure 19b. By comparing the voltages measured at constant current on cracked and uncracked specimens, in principle, electric potential theory can be used to precisely calculate the crack depth. In practice, however, it has been found more convenient to calibrate the probe using a reference flaw, i.e., a machined slot which simulates the anticipated crack size, shape and location. The AC approach circumvents the difficulties associated with the generation of thermal emf's. encountered in the conventional DC approach. Adequate penetration depth is obtained with the AC method by using low frequency (100 Hz), and synchronous detection is used to discriminate against incoherent noise, resulting in much greater sensitivity than can be obtained with the DC technique. This greater sensitivity permits the use of very small drive currents, on the order of 16 ma.

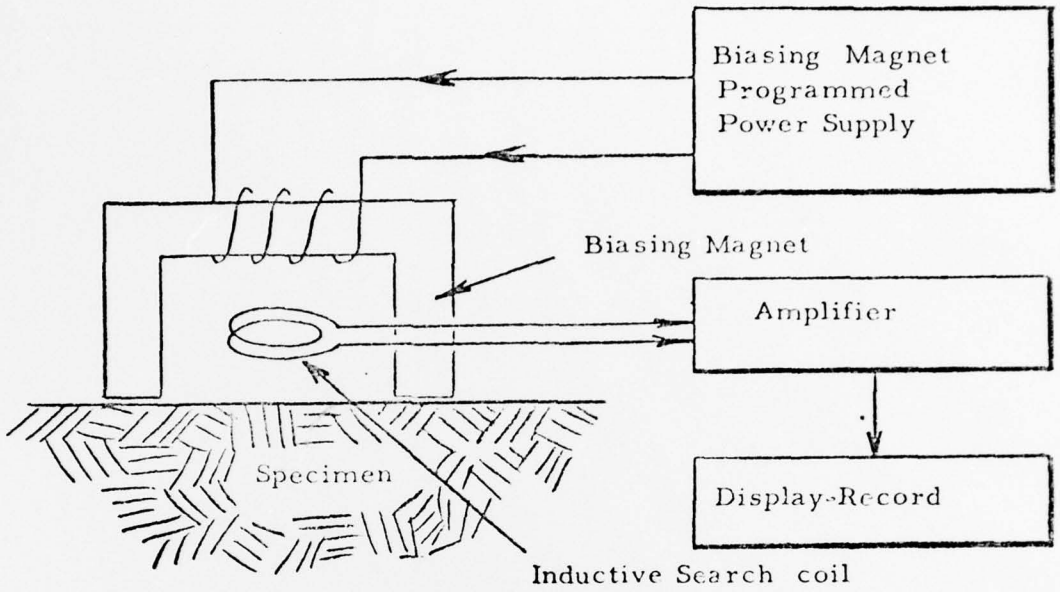

1959

FIGURE 17. SCHEMATIC DIAGRAM OF THE ESSENTIAL FEATURES OF AN ARRANGEMENT FOR INDUCTIVELY SENSING THE BARKHAUSEN EFFECT

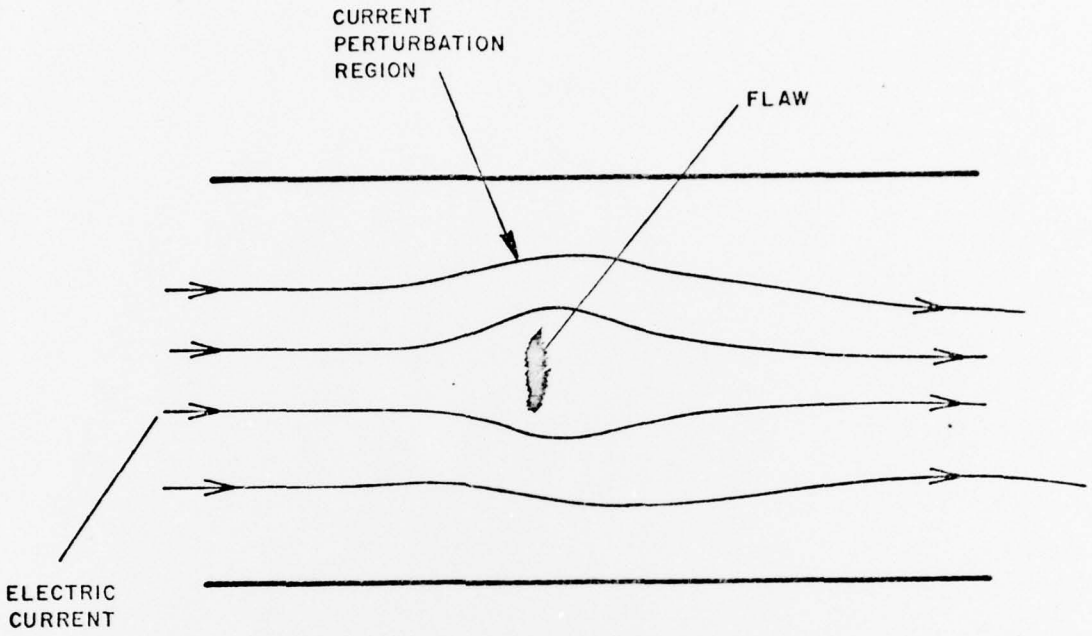

1641

FIGURE 18. ELECTRIC CURRENT INJECTION METHOD
Influence of a Flaw on Electric Current
Distribution

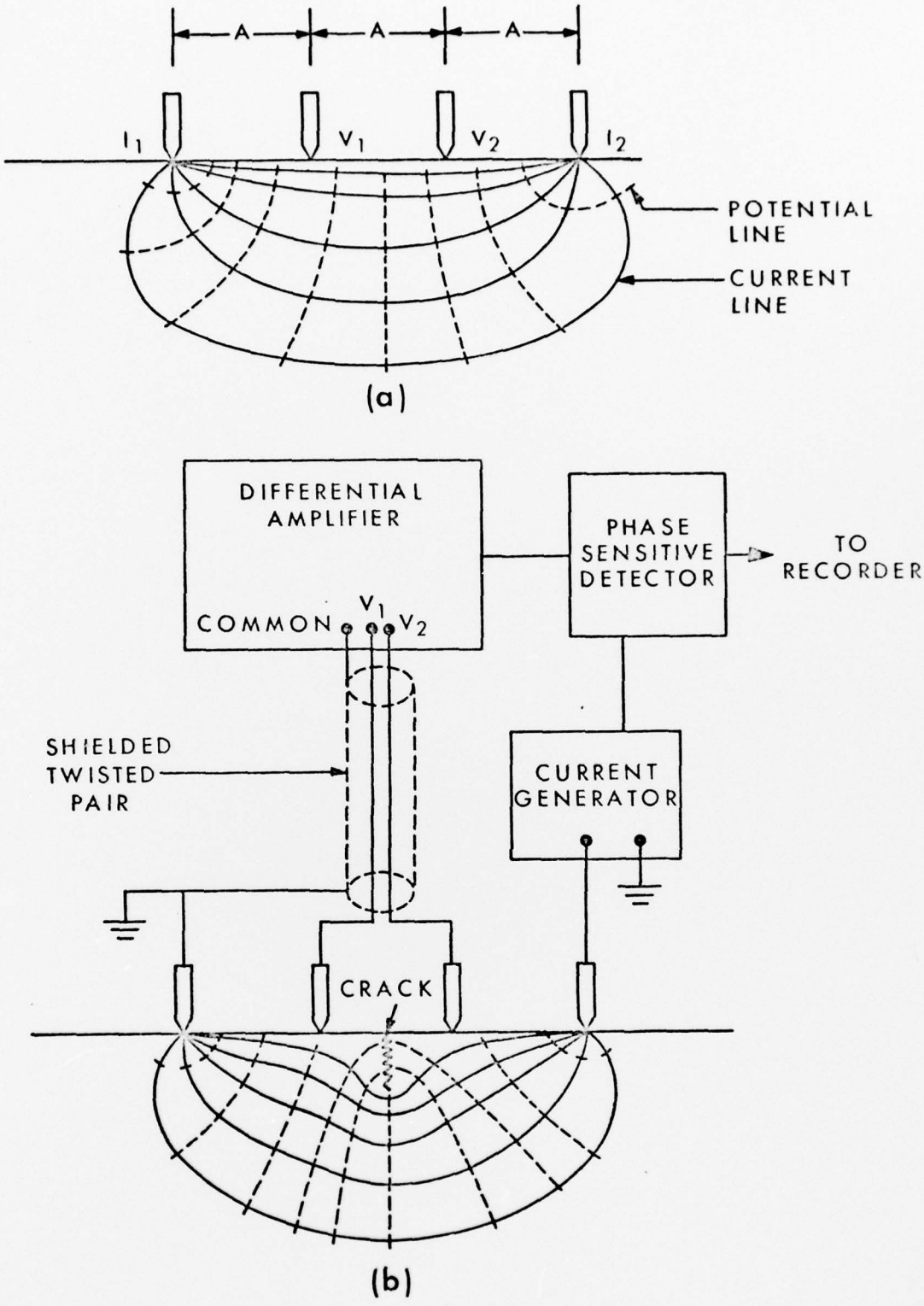

3358

FIGURE 19. OPERATION OF AC FOUR CONTACT ELECTRIC PROBE (a) ON UNCRACKED AND (b) ON CRACKED MATERIAL. The current contacts I_1 and I_D are driven by a current generator. The signal from the voltage contacts V_1 and V_2 is amplified and synchronously detected.